ELSEVIER

Journal of Chromatography A, 762 (1997) 113–133

JOURNAL OF CHROMATOGRAPHY A

Characterisation of silica-based heparin affinity sorbents from equilibrium binding studies on plasma fractions containing thrombin[1]

M. Björklund, M.T.W. Hearn*

Centre for Bioprocess Technology, Department of Biochemistry and Molecular Biology, Monash University, Wellington Road, Clayton, Victoria 3168, Australia

Abstract

The binding properties of rigid heparin sorbents, synthesised by end-point-attachment of heparin onto aminopropyl-derivatised silica through reductive amination, were characterised through batch-adsorption studies employing human plasma fractions containing thrombin. Thrombin was quantified using a chromogenic assay that had been specially modified for these studies. These investigations yielded information regarding the maximum adsorption capacities/stoichiometries and binding affinities for thrombin present in complex protein mixtures. Of the two types of heparin–silica evaluated, heparin–Fractosil 1000, with a pore size of 1000 Å, displayed a capacity of 2.4 mol of thrombin/mol of heparin (mol T–mol H). This stoichiometry was significantly higher than the value of 1.8 mol T–mol H obtained for the commercial soft gel heparin–Sepharose CL-6B. Furthermore, the heparin–Fractosil 1000 sorbents were superior in capacity and binding site accessibility to heparin–LiChroprep Si60 sorbents, where the smaller pore size of 60 Å largely restricts the ligand–protein interactions to the outer surface of the sorbent particles. Nevertheless, heparin–LiChroprep Si60 sorbents were useful, in that they simulated a non-porous particle system, in which intra-pore diffusion effects are eliminated. The batch adsorption results with these sorbents indicated that the adsorption involved both high and low binding affinity characteristics. This bimodal binding mechanism was also evident with the commercial heparin–Sepharose sorbent. Binding stoichiometries and affinities in the high concentration range were similar to values reported for a largely non-specific electrostatic thrombin–heparin interaction. Dissociation constants in the nanomolar range were observed in the low concentrations range. This stronger binding affinity is more similar to highly specific bio-affinity interactions. Thus, the results indicated that heparin–thrombin interactions with these systems involve both a weak electrostatic and a strong biospecific interaction component.

Keywords: Affinity adsorbents; Heparin–silicas; Stationary phases, LC; Thrombin; Proteins

1. Introduction

The synthesis of heparin affinity sorbents [1–3] has involved several different approaches over the years. Initially, heparin was immobilised onto cyanogen bromide (CNBr)-activated Sepharose [4–7], or conversely, CNBr-activated heparin immobilised on an underivatised support [8]. Affinity sorbents based on the CNBr-activation chemistry exhibit limited stability, due to the lability of the chemical bonds of the attachment sites. Furthermore,

*Corresponding author.

[1]Part CLXXI of the series High-performance liquid chromatography of amino acids, peptides and proteins. For Part CLXX, see Ref. [43].

PII S0021-9673(96)00957-0

the heparin molecules are coupled in a randomly oriented manner [6,9]. Since specific heparin–protein interactions involve functional side groups on the heparin carbohydrate chain, these modes of immobilisation could potentially restrict the accessibility of specific binding sites on the heparin molecule to proteins. The general trend has therefore been to use alternative immobilisation chemistries involving end-point-attached heparin. This can be achieved by coupling the heparin through reductive amination onto an aminopropyl-functionalised support, utilising the aldehyde group present at the reducing end of the heparin molecule [1,10]. Soft gel support materials, such as Sepharose, have often been employed for this purpose. One major drawback with these support materials is their relatively low rigidity, which limits the maximum allowable back pressures in liquid chromatography systems, and thereby the possible flow-rates. Soft gel supports are therefore less suitable for use in HPLC applications than rigid materials such as silica [11]. Based on these considerations, a range of rigid heparin sorbents were synthesised by end-point-attachment of non-degraded heparin of a wide molecular mass range onto silica through reductive amination. The use of non-degraded heparin was a preferred option, as this choice was anticipated to most likely result in better preserved ligand multifunctionality and, consequently, offer a wider range of possible protein interaction selectivities with the sorbents.

A well-known heparin–protein specificity involves the interaction of heparin with the mammalian plasma coagulation factors and anti-coagulation factors. Affinity chromatography on immobilised-heparin sorbents has been used for over two decades to purify thrombin [5,7,12,13]. Binding competition, such as the heparin-facilitated desorption of thrombin from heparin–Sepharose, has further been studied through recycling partition equilibrium studies [14]. Heparin affinity chromatography has also been used as a tool in studies aimed at elucidating the coagulation inhibition mechanisms mediated through the antithrombin III (AT III)–thrombin–heparin interaction [15,16]. The thrombin–heparin interaction is easily monitored, since thrombin is readily assayed using the chromogenic synthetic peptide substrate, S2238 [17,18]. These examples demonstrate the usefulness of thrombin as a model protein in the evaluation of heparin affinity sorbents.

Studies on protein–ligand interactions commonly involve pure protein samples [19]. Thus, the performance of soft gel heparin sorbents has often been evaluated using pure thrombin preparations [6,9,10]. In work with rigid heparin sorbents, both pure [20] and crude thrombin preparations [21] have been used. Since the purpose of the present investigations was to evaluate the potential use of rigid heparin sorbents in authentic purification situations, complex protein mixtures were chosen.

2. Experimental

2.1. Chromatographic supports

Heparin Sepharose CL-6B was obtained from Pharmacia (Uppsala, Sweden). LiChroprep Si60 (25–40 and 40–63 μm) and Fractosil 1000 (40–63 μm) were obtained from E. Merck (Darmstadt, Germany).

2.2. Chemicals

The chromogenic peptide substrate (S2238) [17,18,22] used in the thrombin assay was obtained from Chromogenix (Stockholm, Sweden). The protein assay reagent used in the total protein assay was a Dye Reagent Concentrate, from Bio-Rad (Richmond, CA, USA).

2.3. Preparation of affinity sorbents

2.3.1. Aminopropyl-derivatisation of silica [23]

γ-Aminopropyltriethoxysilane (1.88 ml) was added to freshly distilled toluene (300 ml). Fractosil 1000 with a particle size of 40–63 μm (50 g), pre-dried under high vacuum for 12 h at 180°C was then added. The suspension was sonicated for 1 min and refluxed for 12 h at 150°C. The aminopropyl-derivatised silica was then washed with toluene (200 ml) followed by isopropanol (150 ml) and finally dried at 110°C.

2.3.2. Coupling of heparin to aminopropyl-derivatised silica

Heparin (approximately 10–200 and 50–1000 mg/g silica for LiChroprep Si60 and Fractosil 1000, respectively) was dissolved in 0.2 *M* potassium

phosphate buffer, pH 7.0 (5 ml/g silica). Dry silica and $NaCNBH_3$ were then added (0.1 mg $NaCNBH_3$/mg heparin). The slurry was degassed for 5 min with careful swirling and then allowed to react at room temperature for 60–70 h with end-over-end mixing using a rotary suspension mixer. The sorbent was washed on a glass sinter funnel with 0.2 *M* potassium phosphate buffer, pH 7.0, water and 0.2 *M* sodium acetate (40 ml of each per g of sorbent), and then suspended in 0.2 *M* sodium acetate (40 ml/g sorbent). Unreacted amines were acetylated by sequential addition of acetic anhydride at 2-min intervals over 6 min (4 times 0.25 μl/mg sorbent) with vigorous stirring using a suspended impeller. The pH during the blocking step was kept between 7 and 8 by titration with 5 *M* NaOH. The reaction was continued for an additional 4 min after the last addition of acetic anhydride. The sorbent was finally washed with a 0.2 *M* sodium acetate solution, pH 5 (40 ml/g sorbent), and stored at +4°C in the same buffer.

2.4. Preparation of thrombin material

Thrombin was donated by CSL (Parkville, Australia) in an inactive (prothrombin) frozen form designated "prothrombin cut", or PTX. The thawed PTX material was activated at 37°C with thromboplastin and thromboplastin solution (15 ml, extracted from placentae, per 100 ml of PTX) was added. 0.80 *M* $CaCl_2$ (3.5 ml per 100 ml of PTX) was then added dropwise with continuous mixing. The mixture was allowed to react for 3 h at 25°C with brief swirling once every hour, then filtered through three layers of dry gauze and dialysed against 0.01 *M* Tris–0.15 *M* NaCl, pH 7.5, using 8000 M_r cutoff, 32 mm dialysis tubing (Union Carbide) at 4°C. Dialysed material, designated as batches B056, B062, B995 and B998, was stored at −20°C in 2, 5 or 10 ml aliquots.

2.5. Characteristics of thrombin materials

The thrombin amidolytic activities and specific activities in the starting material batches used in these studies are shown in Table 1. The protein compositions of the B056, B995 and B998 starting materials were similar, as was evident from sodium dodecyl sulphate–polyacrylamide gel electrophoretic (SDS–PAGE) analysis. In contrast, the very low specific activity of batch B062 was accompanied by a considerably larger proportion of high-molecular-mass material, together with a less intense thrombin band (M_r 36 600). S2238-specific amidolytic activities due to other proteases were found to be negligible in these batches, as determined through activity assays in the presence of hirudin, a thrombin-specific polypeptide protease inhibitor prepared from leeches (*Hirudo medicinalis*).

2.6. Thrombin assay

Thrombin was quantified in terms of its proteolytic activity with the chromogenic substrate S2238 [17,18,22] by measuring the colour formation rate at 405 nm. Samples were diluted in assay buffer (20 m*M* Tris–0.1 *M* NaCl–0.01% Brij 35, pH 8.0) to obtain a colour formation rate ranging between 0.02 and 0.2 A.U./10 min. Typically, a thrombin standard that contained 578 U/ml was diluted 1:1000. The reconstituted substrate, S-2238 (H-D-Phe-Pip-Arg-pNA, 1 m*M* in 0.01% Brij 35) was stored frozen in 500 μl aliquots and was diluted 1:5 in assay buffer immediately before use. In the assay, diluted samples

Table 1
Specific activities of thrombin in the starting materials

Thrombin batch	Protein (mg/ml)	Thrombin (U/ml)	Specific activity (U/mg)
B056	26.2 (±16%)	5300 (±6%)	200
B995	23.0 (±11%)	3700 (±15%)	150
B998	17.2 (±10%)	1640 (±5%)	95
B062	13.4 (±10%)	43.0 (±7%)	3.2

The specific activities of the four thrombin batches used in these investigations were determined from the specific thrombin activity and total protein assays.
Percentile inter-assay variations are indicated.
Activity data are given to two significant figures.

(20 μl) were placed in the wells of a 96-well flat bottom microtitre plate (Greiner Labortechnik, Frickenhausen, Germany) and the diluted substrate (50 μl) was added (at time 0) to the wells in rapid sequence using an Eppendorf multipipette. The absorbance at 405 nm was then measured automatically at 2 min intervals with the aid of a model 3550 Microplate reader (Bio-Rad, Japan). Sample readings were plotted against time, generating individual colour formation rates through first order linear regression. The slopes were thus easily visualised and the linear range of the colour formation reaction was selected. Colour formation rates were converted to thrombin activities relative to a thrombin standard material containing 578 U/ml (±2.1%), which was included in the assays. The standard material (2500 U/bottle, donated by CSL) was calibrated in this laboratory against an accurate thrombin standard containing 83 U/bottle (donated by CSL). The thrombin activities in the samples were related to the standard material (diluted 1:1000) using the formula:

$$\mathrm{U/ml} = \frac{R(D_s) \cdot 578}{R_{std} \cdot 1000} \quad (1)$$

where, R = sample colour formation rate − background rate; R_{std} = standard colour formation rate − background rate and D_s = sample dilution.

Linear regression analysis of the assay data for the 578 U/ml thrombin standard diluted between 1:500 and 1:20 000 indicated that the standard curve was linear through this dilution interval ($r = 0.9975$). The lower limit of sensitivity using the assay system was 0.03 U thrombin/ml.

2.7. Total protein assay

The assay procedure used was a modified version of the Bio-Rad dye binding assay, adapted as part of these investigations specifically for microtitre plate measurements. As protein standards, bovine serum albumin (BSA) was diluted to 0.01, 0.025, 0.05, 0.125 and 0.25 mg/ml in 0.01 *M* Tris–0.15 *M* NaCl, pH 7.5 (buffer A). Unknown samples were diluted between 1:1 and 1:100 in the same buffer. The diluted standard or sample (0.1 ml) was then mixed with distilled water (0.7 ml), and undiluted Bio-Rad Coomassie reagent (0.2 ml) was added. As a blank, buffer A (0.2 ml), distilled water (1.4 ml) and reagent (0.4 ml) were mixed. All mixtures were then vortex-mixed and 200 μl volumes were pipetted into a 96-well flat bottom microtitre plate (Greiner Labortechnik). The blank mix was placed in column 1 on the plate. The absorbance at 595 nm was measured on a Titertech Multiskan MCC/340 microplate reader (Flow Labs., Helsinki, Finland) and protein concentrations of the samples were read from the standard curve using a linear regression program.

2.8. Batch adsorption experimental set-up

Approximately 50% (v/v) suspensions of heparin sorbent equilibrated in 0.01 *M* Tris–015 *M* NaCl, pH 7.5 (adsorption buffer), were pipetted into 1 ml disposable syringes with tips removed. The adsorbent aliquots were packed by spinning the syringes for 1 min in a bench-top centrifuge. Excess buffer was removed carefully using a Pasteur pipette, and settled sorbent volumes (between 0.050 and 0.200 ml) were determined from the syringe grading. The adsorbent aliquots were then transferred into reaction vessels (5 or 10 ml polypropylene scintillation vials). Thrombin-containing material was diluted in adsorption buffer to between 1:5 and $1:10^5$ for thrombin batches B056, B995 and B998, and 1:2 to 1:100 for batch B062. Diluted protein solution (5 ml, with the exact amount determined by mass) was incubated with duplicate adsorbent aliquots in the reaction vessels overnight on a rotary suspension mixer in a refrigerated incubator (Thermoline, Smithfield, Australia) at 25.0°C. Samples of starting material were incubated under identical conditions. The adsorbent aliquots were then settled at 25.0°C by brief centrifugation (4500 *g* for 5 min on a Sorvall RT6000 bench-top centrifuge) and samples of supernatants were removed immediately. Supernatants and starting materials were assayed for thrombin content in a chromogenic assay using substrate S-2238.

2.9. Evaluation of equilibrium binding data

The equilibrium concentrations of bound thrombin (q^*) were derived from the measured thrombin concentrations (c^*) in solution (supernatants) at equilibrium as follows:

c^* = thrombin activity in supernatant (U/ml) (2)

and

$$q^* = \frac{C_0V - [c^*(V + f_{liq}v_s)]}{v_s} \text{ (U/ml sorbent)} \quad (3)$$

where, C_0 = initial thrombin activity in the starting material; V = volume of added protein solution; f_{liq} = liquid fraction in settled sorbent (ml/ml sorbent) and v_s = settled volume of sorbent.

The liquid fractions, or the proportion of a volume of settled sorbent which is taken up by liquid (f_{liq}), were calculated using characteristic weight–volume relationships for each support material, determined in this laboratory as described elsewhere [24]. The f_{liq} values for support materials used in these experiments are shown in Table 2.

Apparent maximum capacities, q'_m, and apparent dissociation constants, K'_d (expressed in units of thrombin per ml of sorbent), were determined through first-order curve-fits of the data points using double reciprocal-, Scatchard- and Scott (semi-reciprocal) plots. Adsorption isotherms corresponding to the equations of these linear regressions were then generated. Apparent capacities and dissociation constants were then converted to molar quantities using the average molecular mass of heparin, 13 500 g/mol [25]; the molecular mass of human α-thrombin, 36 600 g/mol [26]; the immobilised heparin contents on the sorbents (mg H/ml sorbent) and the average specific activity of 2346 U/mg for highly purified thrombin achieved in this laboratory [27]. This value was similar to values for pure thrombin reported by other investigators [7,21,28,29]. Heparin contents of the affinity sorbents are given in Table 2.

2.10. Experimental configuration

Four different thrombin-containing materials, batches B995 (3675 U/ml), B056 (5279 U/ml), B062 (43 U/ml) and B998 (1638 U/ml) were used in batch adsorption studies using heparin–LiChroprep Si60, heparin–Fractosil 1000 and commercial heparin–Sepharose sorbents. A summary of the various combinations of thrombin material–heparin–sorbent is given in Table 3.

Mesoporous heparin–LiChroprep Si60 sorbents of two different particle size ranges (25–40 and 40–63 μm) were compared, using the HLC 19 and HLC 20 sorbents, respectively. The LiChroprep Si60 sorbents with 25–40 μm particle size, and with four different heparin contents–ligand densities (HLC 21a–HLC 21d), were also studied using high- (batch B056) and low thrombin activity (batch B062) starting materials. Due to the small pore size of the LiChroprep Si60 particles (60 Å), the adsorption capacity of sorbents based on this silica material is, however, limited. The macroporous Fractosil 1000 (pore size 1000 Å) was therefore the logical choice for the further development of a rigid heparin sorbent. A heparin–Fractosil 1000 sorbent with 40–63 μm particle size (HFS 13), containing 4.15 mg of

Table 2
Liquid fractions and immobilised heparin contents of heparin–LiChroprep Si60, heparin–Fractosil 1000 and heparin–Sepharose

Support material	f_{liq} (ml/ml$_s$)	Sorbent	mg H/ml sorbent
LiChroprep Si60 (25–40 μm)	0.726	HLC 19	1.64
LiChroprep Si60 (40–63 μm)	0.748	HLC 20	1.70
LiChroprep Si60 (25–40 μm)	0.726	HLC 21a	0.29
		HLC 21b	1.12
		HLC 21c	2.56
		HLC 21d	8.58
Fractosil 1000 (40–63 μm)	0.719	HFS 13	4.15
Sepharose	0.964	Comm HS	2.64

Liquid fractions (f_{liq}) were calculated based on the specific mass–volume relationships of the batch adsorption system determined for each support material.

The heparin contents (mg H/ml sorbent) of the affinity sorbents were determined through a modified spectrophotometric method [24] for the determination of hexosamines.

f_{liq} = liquid fraction in settled sorbent; ml$_s$ = volume settled sorbent; H = heparin; HLC = heparin–LiChroprep Si60; HFS = heparin–Fractosil 1000; Comm HS = commercial heparin–Sepharose.

Table 3
Experimental configurations used with the various thrombin batches and heparin–sorbents

Thrombin batch	Sorbent	Particle size range (μm)
B995	HLC 19	25–40
	HLC 20	40–63
	Blank	25–40
		40–63
B056	HLC 21a–d	25–40
	Blank	
B062	HLC 21a–d	
	Blank	
B998	HFS 13	40–63
	Blank	
	CHS	
	Blank	

Heparin–LiChroprep Si60 sorbents (HLC) of particle size 25–40 and 40–63 μm, heparin–Fractosil 1000 sorbents (HFS) of particle size 40–63 μm, commercial heparin–Sepharose (CHS) and corresponding blank support materials were studied in various combinations with thrombin batches B995, B056, B062 and B998, as indicated in this table.
"Blank" refers to the non-heparin-derivatised (non-coupled, but acetylated and amino-derivatised) support material.

heparin per ml of sorbent, was chosen for batch adsorption studies with thrombin. A comparison was made with commercial heparin–Sepharose at 25°C; the performance of the HFS 13 sorbent was studied in a similar manner at 4 and 37°C. Thrombin starting material (batch B998 diluted in 0.01 *M* Tris–0.15 *M* NaCl, pH 7.5) was pre-equilibrated at these temperatures prior to batch adsorption with the sorbent aliquots. The effect of thrombin concentration was studied in terms of adsorption isotherms, generated by using a series of different thrombin concentrations in the dilution range 1:2 to 1:1000. Initially, 5 ml volumes of diluted starting material were used; larger volumes, 8 and 14 ml of 1:2 dilutions, were however also required in order to reach the upper parts of the adsorption isotherms (saturation of the sorbent). The effect of non-specific adsorption was studied using non-coupled, acetylated amino-derivatised support material. This background adsorption was, however, found to be negligible compared to the thrombin interaction with heparin affinity sorbents.

3. Results and discussion

3.1. Batch adsorption experiments with heparin–LiChroprep Si60 sorbents

3.1.1. Two-mode interaction

Quantitative analysis of the batch adsorption data for the thrombin preparations with the heparin–Lichroprep Si60 sorbents using double reciprocal, Scatchard, and Scott plots revealed that the data could not be fitted to a simple linear dependency (1^{st} order regression). As exemplified in Fig. 1, distinctly different slopes in the linearisation plots were evident at both low and high thrombin concentrations. This result suggested that the adsorption mechanism was not of a single component Langmuir type, but rather that at least two classes of binding processes were participating. The possibility that this result could have been an artefact due to reduced accuracy in the assay at low thrombin concentrations can be eliminated, since the majority of the values in the lower concentration range were well above the lower sensitivity limit of the thrombin assay (0.03 U/ml). The two slopes in the linearisation plots can thus be considered to reflect manifestations of two different adsorption phenomena, with the first mode of interaction becoming less dominant at a c^*-value of approximately 0.5 U/ml, or a q^* value of 500 U/ml.

The q_m and K_d values representing the two different interaction modes were determined by analysing the data from the upper and lower parts of the plots separately. Values obtained using the three different linearisation plots generally coincided well (see Table 4) and yielded correlation coefficients that predominantly had values higher than 0.9 for the individual plots. The two different modes of interaction could thus be approximated individually as single component Langmuir-type isotherms, even though the interaction as a whole had a non-Langmuirean character. This result indicated that competing binding mechanisms exist with these heparin–silica sorbents, with the overall binding behaviour describable in terms of two competing (Langmuir-type) isotherms.

As evident from Table 5, the stoichiometries and binding affinities for the thrombin–heparin (T:H) interaction differed significantly between the low and

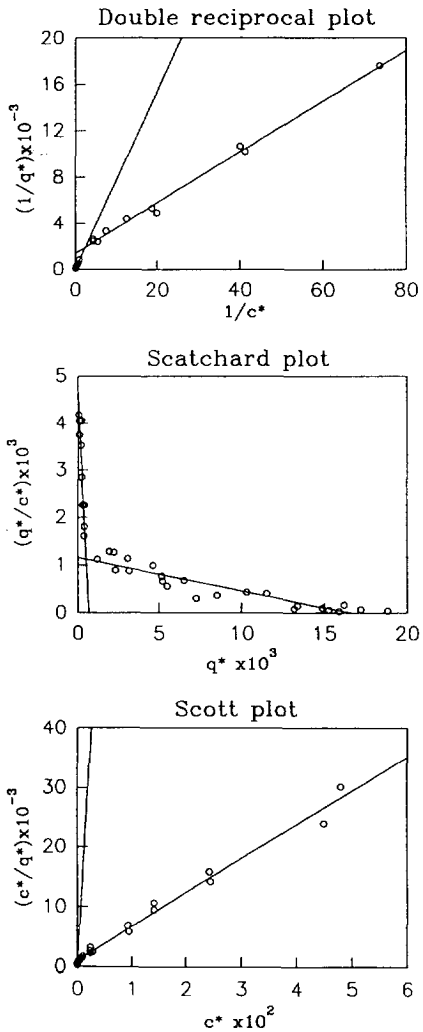

Fig. 1. Linearisation plots for the adsorption isotherm with the HLC 19 adsorbent using thrombin batch B995. The two modes of interactions were visualised through double reciprocal, Scatchard and semi-reciprocal (Scott) plots of the experimental adsorption data.

high concentration ranges. Thus, thrombin bound to the HLC 19 sorbent at a ratio of 1.55 mol T–mol H, with a dissociation constant of 0.17 μ*M* in the high concentration range; in the low range, the molar ratio was only 0.065 mol T–mol H, whilst the dissociation constant of ca. 2 n*M* indicated a 100-fold stronger binding affinity. Dissociation constants in the high concentration range were similar to literature values for a mainly non-specific electrostatic interaction between thrombin and heparin. For example, Olson [30] reported an apparent dissociation constant of 0.69±0.06 μ*M* as determined from equilibrium binding studies. A similar value of $8 \cdot 10^{-7}$ *M* was reported by Jordan et al. [31]. Winzor et al. [14] reported an affinity constant of $1.7 \cdot 10^{6}$ M^{-1} (translating to a K_d of $5.9 \cdot 10^{-7}$ *M*) for the thrombin–heparin interaction using recycling partition experiments involving the displacement of thrombin from heparin–Sepharose by soluble heparin. Evington et al. [32] observed a dissociation constant of 0.2–2 μ*M* in equilibrium titration studies, and 1–3 μ*M* from fluorescence polarisation measurements [33]. Binding stoichiometries have been reported as being in the range 2.4 to 6.8 mol T–mol H [34]; 1 to 2.9 mol T–mol H [35] and 2:1 mol T–mol H [31]. These values corresponded well with our results in the high concentration range.

Binding affinities in the low protein concentration range were indicative of dissociation constants in the nanomolar range, very similar to strong specific bioaffinity interactions such as antibody–antigen binding. A dissociation constant of $1.7 \cdot 10^{-9}$ *M* for the thrombin–heparin interaction has been reported by Griffith et al. [36,37]. This value was arrived at indirectly through studies involving the enhancing effect of heparin on the binding of thrombin to a synthetic tripeptide anilide substrate. Furthermore, Byun et al. [38] reported an affinity constant of $1.76 \cdot 10^{8}$ M^{-1} for the binding of thrombin to heparin immobilised onto polymer-coated glass beads. This value translates to a K_d of $5.68 \cdot 10^{-9}$ *M*. A possible explanation for this nanomolar range of the K_d values with the low concentration range adsorption would be the existence of low abundance, but high affinity binding sites on heparin, which are rapidly exhausted with very low thrombin concentrations, with the greater proportion of the binding (at higher concentrations) occurring through the more commonly observed, but weaker, non-specific electrostatic interactions. An alternative explanation for multiple modes of thrombin–heparin interaction relies on the existence of more than one heparin binding site on thrombin. A second, weaker, binding site on thrombin for heparin has been suggested by Olson et al. [35]. The probability of one thrombin molecule

Table 4
Equilibrium data for the batch adsorption of thrombin with HLC 19 and HLC 20 sorbents

	q'_m (U/ml sorbent)	K'_d (U/ml sorbent)	Stoichiometry (mol T–mol H)	K_d (μM)	Correlation coefficient
HLC 19 (1.64 mg heparin/ml sorbent)					
Low range plot					
Double reciprocal	710	0.16	0.068	0.002	0.997
Scatchard	680	0.15	0.065	0.002	−0.922
Scott	630	0.13	0.060	0.002	0.976
High range plot					
Double reciprocal	14 170	10.9	1.36	0.13	0.988
Scatchard	16 630	14.4	1.59	0.17	−0.931
Scott	17 600	19.0	1.69	0.22	0.994
HLC 20 (1.70 mg heparin/ml sorbent)					
Low range plot					
Double reciprocal	936	0.25	0.087	0.003	0.991
Scatchard	1048	0.28	0.097	0.003	−0.750
Scott	1000	0.27	0.093	0.003	0.897
High range plot					
Double reciprocal	15 400	28.6	1.42	0.33	0.958
Scatchard	16 800	35.4	1.56	0.41	−0.838
Scott	16 600	43.0	1.54	0.50	0.977

Thrombin batch B995 (3675 U/ml) was used in these studies. The initial values, expressed in terms of activity units per volume, were converted to molar values, as described in the text.
Data generated using three different linearisation plots (double reciprocal, Scatchard and semi-reciprocal/Scott) are shown. The first-order linear correlation of the data to these plots is shown in the last column. The data have been divided into "high" and "low" protein concentration ranges, representing the two modes of interaction that were observed using a high thrombin content material.
T = thrombin, H = heparin

binding to more than one ligand would thus increase with the ligand density, thereby influencing the binding stoichiometries and affinities.

3.1.2. Particle size effects

When comparing the adsorption isotherms for heparin–LiChroprep Si60 sorbents of two particle sizes, 25–40 μm (HLC 19) versus 40–63 μm (HLC 20), no significant differences in capacity were observed, when experimental errors of the system were taken into consideration (see Fig. 2). This observation was confirmed by the similar stoichiometry determinations (see Tables 4 and 5). Thus, 1.55 mol T and 1.51 mol T was bound per mol H in the

Table 5
Average molar equilibrium values

Sorbent	Low concentration range		High concentration range		Heparin content (mg/ml sorbent)
	Stoichiometry (mol T–mol H)	K_d (μM)	Stoichiometry (mol T–mol H)	K_d (μM)	
HLC 19	0.065	0.002	1.55	0.17	1.64
HLC 20	0.092	0.003	1.51	0.42	1.70

Averages of molar values in the low and high concentration ranges obtained using the three different linearisation plots (see Table 4) are shown.
T = thrombin, H = heparin

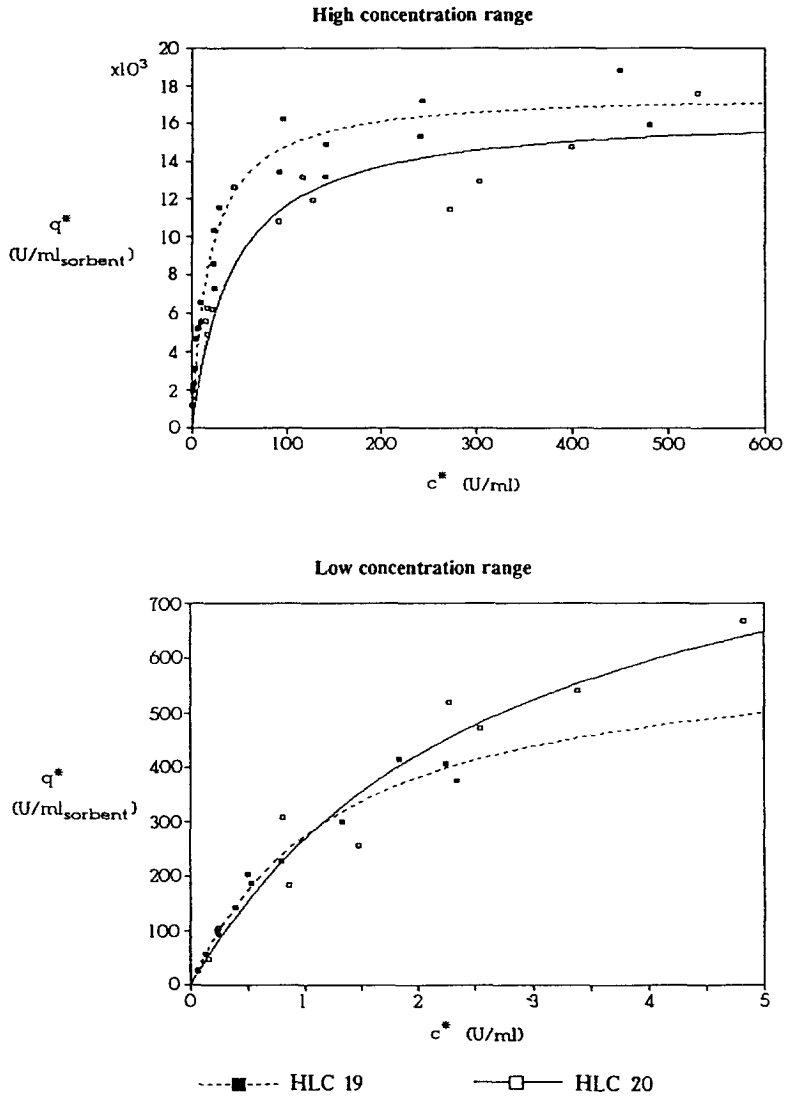

Fig. 2. Adsorption isotherms for the HLC 19 and HLC 20 sorbents with thrombin. The isotherms were fitted to the data points using the computer software written for this purpose and used for calculation of the equilibrium parameters (see text). Isotherms for the high and low concentration ranges of the thrombin–heparin interaction are shown in the top and the bottom graph, respectively.

high thrombin concentration range for the small and the large particles, respectively. With a smaller accessible outer surface area on the larger particles [24], and similar contents of heparin being measured on the two particle sizes, a higher ligand coverage on the large particles was anticipated. This higher ligand density could theoretically result in a lower capacity on the large-particle sorbent (HLC 20), due to the shielding of binding sites on the heparin molecule. The data, however, suggested that no such steric hindrance was occurring.

A geometrically based prediction of the accessible outer surface area of the modified Lichroprep Si60 adsorbent may, however, be an over-simplification. Although the heparin–LiChroprep Si60 sorbents are mesoporous, and protein–ligand interactions therefore are not likely to occur within the pore network, the space occupied by pore openings will influence

the total outer-surface area. Since both support materials (small- and large particle size) have the same pore size (60 Å), the reduction of total outer-surface area due to pore openings would theoretically be greater for the smaller particle size silica. If this effect is prominent enough to cancel out the theoretically larger outer-surface area on the small particles, it could result in the similar capacities observed in these studies.

Furthermore, in the low concentration range, the capacity of the large particle size sorbent was actually significantly higher than that found with the small particle size, as seen from the stoichiometries in Table 5 of 0.092 and 0.065 mol T–mol H for HLC 20 and HLC 19, respectively. Quantitative data, however, indicated an overall lower affinity with the large particle size. This result could possibly indicate a reduced binding site accessibility due to a higher ligand density with the larger particles. The measured heparin contents on the heparin–LiChroprep Si60 sorbents (see Table 2) suggested that steric effects due to the close proximity of the polysaccharide chains would most likely be prominent [24]. Such ligand density-dependent effects are not uncommon and have, for example, been observed in dye–ligand–protein interactions [39].

3.1.3. Ligand density effects

An overall trend with two modes of interaction was observed at four different ligand densities on the heparin–LiChroprep Si60 sorbents of 25–40 μm particle-size (HLC 21a–HLC 21d) when using the B056 thrombin starting material batch. For the quantitative analysis, the data were therefore divided into high and low protein concentration ranges, as described earlier.

Adsorption isotherms describing the interaction in terms of U thrombin/ml sorbent are shown in Fig. 3. A clear correlation to heparin content is seen, as expected. Binding stoichiometries (mol T–mol H) were found to be inversely proportional to heparin content in both protein concentration ranges (see Table 6). This result indicated a reduced accessibility of thrombin binding sites with increased ligand density, probably due to steric effects. The reduction in mol T–mol H stoichiometry was most prominent between the sorbent with the lowest (HLC 21a) and the second lowest (HLC 21b) heparin content; a three-fold reduction in the low concentration range and a two-fold reduction in the high range. These values closely reflect the 3.8-fold greater heparin content with the HLC 21b sorbent compared to HLC 21a. A further increase in ligand density (with HLC 21c and HLC 21d) caused proportionally much smaller changes in binding stoichiometry. One possible interpretation of this finding would be that the surface area is already close to saturated with heparin ligands with the HLC 21b sorbent [24].

Overall, the differences in capacities and binding affinities between the two concentration ranges were greater with the HLC 21a–HLC 21d sorbents than with the HLC 19 and HLC 20 sorbents. Thus, the HLC 21b adsorbent exhibited a more than 1000-fold higher affinity, together with a 50-fold higher capacity in the high concentration range. This finding is most likely to be due to the complex nature of the starting materials, since different batches of thrombin material were used. As seen in Table 1, the specific activity of batch B056 (used with heparin sorbents HLC 21a–HLC 21d) was 202 U/mg, while that of batch B995 (used with heparin sorbents HLC 19 and HLC 20) was 153 U/mg. These differences in specific activity may reflect the presence of other components that attenuate the thrombin–heparin interaction.

3.1.4. Starting material with low thrombin content

In contrast to the thrombin batches earlier described, batch B062 had a considerably lower specific thrombin activity, i.e. 3.2 U/mg (see Table 1). When using this starting material in batch adsorption studies with the HLC 21a–HLC 21d sorbents, the two-mode interaction was not observed. Capacity and binding affinity values were therefore determined through linear regression analysis of the entire data sets; the values thus calculated are shown in Table 7. Adsorption isotherms describing the interaction in terms of U thrombin/ml sorbent using this thrombin batch are shown in Fig. 4. As can be seen, the maximum q^* values of the isotherms are on an entirely different level compared to the values obtained in the high concentration range using the (high-activity) B056 thrombin batch with these sorbents. Although a correlation between sorbent heparin content and adsorption capacity, similar to that found when using the high-activity batch, was

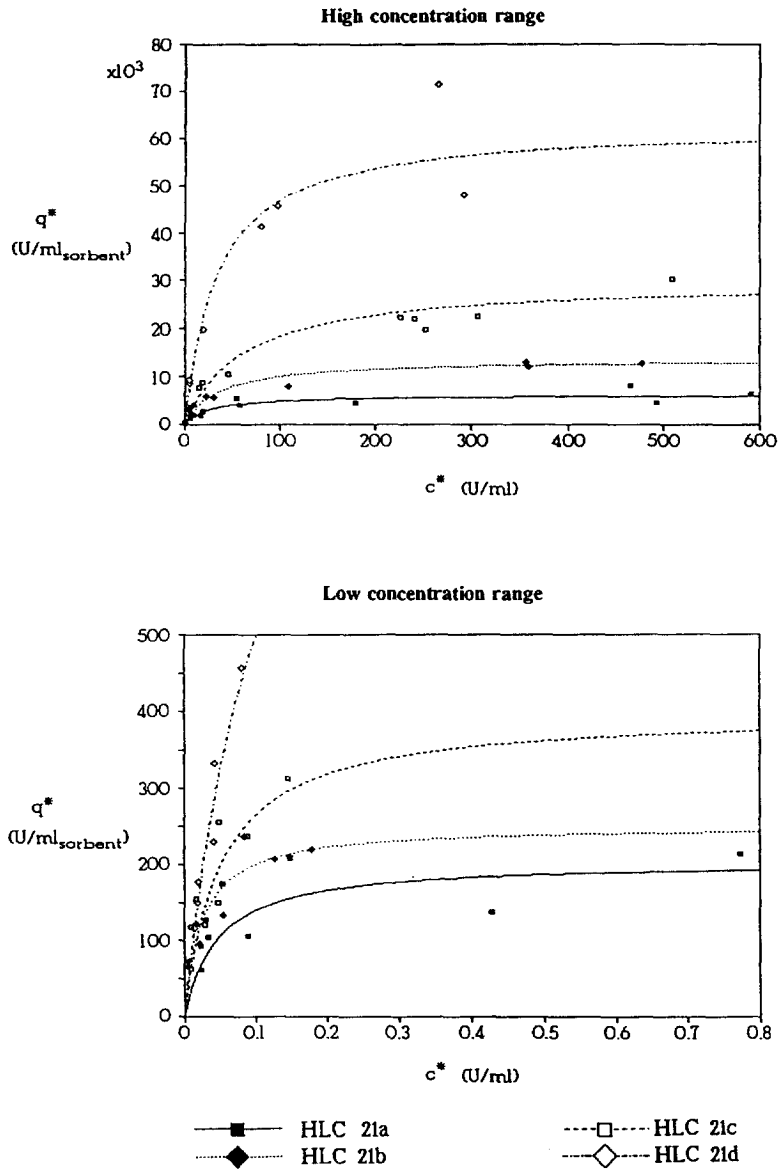

Fig. 3. Isotherms for the adsorption of thrombin with heparin–LiChroprep Si60 sorbents of four different heparin contents (HLC 21a–HLC 21d). Isotherms were fitted to the data points using the computer software written for this purpose and used for the calculation of the equilibrium parameters. Isotherms for the high and low concentration ranges of the thrombin–heparin interaction are shown in the top and the bottom graph, respectively.

evident from the shapes of the isotherms, no clear-cut ligand density dependency on stoichiometry and binding affinity was observed (see Table 8). Overall, the capacities were nevertheless similar to the low concentration range observed with the high-activity thrombin batch. Binding affinities were intermediate to those found for the low and high concentration ranges using the high-activity thrombin material. These observations could indicate the presence of other heparin-binding components in batch B062 that interfered with the thrombin–heparin interaction, or possibly that the thrombin in this batch itself was

Table 6
Equilibrium data for the adsorption of thrombin with the HLC 21a–HLC 21d sorbents

	q'_m (U/ml sorbent)	K'_d (U/ml sorbent)	Stoichiometry (mol T–mol H)	K_d (μM)	Correlation coefficient
HLC 21a (0.29 mg heparin/ml sorbent)					
Low range plot					
Double reciprocal	208	0.04	0.11	0.0005	0.745
Scatchard	356	0.11	0.19	0.0012	0.352
Scott	204	0.05	0.11	0.0006	0.963
High range plot					
Double reciprocal	4840	16.2	2.63	0.19	0.993
Scatchard	6670	26.6	3.62	0.31	0.874
Scott	6170	27.1	3.35	0.32	0.960
HLC 21b (1.12 mg heparin/ml sorbent)					
Low range plot					
Double reciprocal	208	0.02	0.029	0.0002	0.945
Scatchard	260	0.02	0.037	0.0003	0.819
Scott	250	0.03	0.035	0.0003	0.978
High range plot					
Double reciprocal	10 500	16.4	1.48	0.19	0.949
Scatchard	12 600	23.5	1.76	0.27	0.888
Scott	13 500	34.8	1.89	0.41	0.994
HLC 21c (2.56 mg heparin/ml sorbent)					
Low range plot					
Double reciprocal	266	0.023	0.016	0.0003	0.797
Scatchard	470	0.056	0.029	0.0007	0.467
Scott	398	0.051	0.025	0.0006	0.900
High range plot					
Double reciprocal	22 030	24.9	1.35	0.29	0.992
Scatchard	26 230	35.0	1.61	0.41	0.910
Scott	29 800	61.7	1.83	0.72	0.974
HLC 21d (8.58 mg heparin/ml sorbent)					
Low range plot					
Double reciprocal	950	0.099	0.018	0.001	0.983
Scatchard	1270	0.14	0.023	0.002	0.672
Scott	1070	0.11	0.025	0.001	0.800
High range plot					
Double reciprocal	51 800	22.9	0.95	0.27	0.980
Scatchard	66 000	35.4	1.21	0.41	0.887
Scott	63 000	34.0	1.15	0.40	0.958

Starting material was the thrombin batch B056 with a high thrombin content. Thrombin batch B056 (5279 U/ml) was used.
The initial values, expressed in terms of activity units per volume, were converted to molar values as described in the text.
Data generated using three different linearisation plots (double reciprocal, Scatchard and semi-reciprocal/Scott) are shown.
The first-order linear correlation of the data to these plots is shown in the last column.
The data have been divided into "high" and "low" protein concentration ranges, representing the two modes of interaction that were observed using a high thrombin content material.
T = thrombin, H = heparin.

Table 7
Equilibrium data for the adsorption of thrombin with the HLC 21a–HLC 21d sorbents

Plot	q'_m (U/ml sorbent)	K'_d (U/ml sorbent)	Stoichiometry (mol T–mol H)	K_d (μM)	Correlation coefficient
HLC 21a (0.29 mg heparin/ml sorbent)					
Double reciprocal	390	3.69	0.21	0.043	0.909
Scatchard	<0	<0	–	–	–
Scott	106	0.45	0.06	0.005	0.932
HLC 21b (1.12 mg heparin/ml sorbent)					
Double reciprocal	960	4.88	0.13	0.057	0.778
Scatchard	880	3.54	0.12	0.041	−0.295
Scott	670	3.18	0.09	0.037	0.660
HLC 21c (2.56 mg heparin/ml sorbent)					
Double reciprocal	8800	21.8	0.54	0.25	0.946
Scatchard	1370	2.97	0.09	0.035	−0.580
Scott	1250	2.75	0.08	0.032	0.896
HLC 21d (8.58 mg heparin/ml sorbent)					
Double reciprocal	4170	3.38	0.08	0.039	0.992
Scatchard	2450	1.89	0.04	0.022	−0.689
Scott	2310	1.79	0.04	0.021	0.816

Starting material was the thrombin batch B062 with low thrombin content.
Thrombin batch B062 (43 U/ml) was used.
The initial values, expressed in terms of activity units per volume, were converted to molar values as described in the text.
Data generated using three different linearisation plots (double reciprocal, Scatchard and semi-reciprocal/Scott) are shown.
The first order linear correlation of the data to these plots is shown in the last column.
T = thrombin, H = heparin.

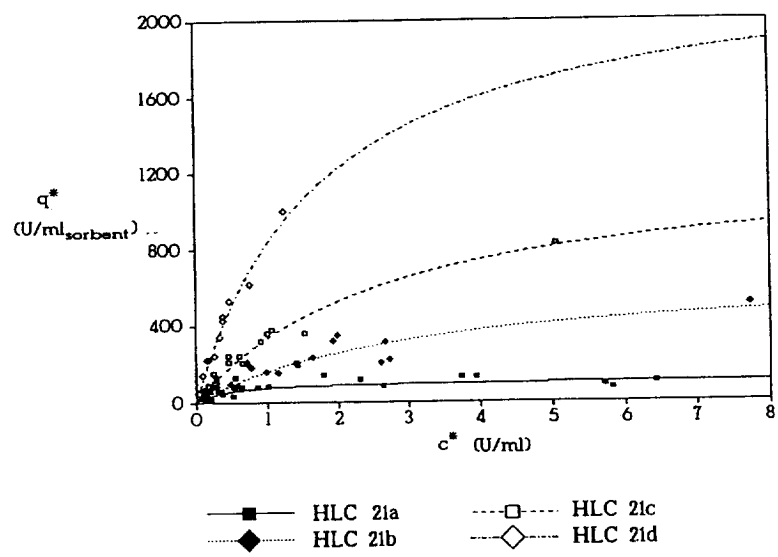

Fig. 4. Adsorption isotherms for the low-thrombin material with the HLC 21a–HLC 21d sorbents. Isotherms were fitted to the data points using the computer software written for this purpose and used for the calculation of the equilibrium parameters (see text).

Table 8
Average molar equilibrium values for the adsorption of thrombin with the heparin–LiChroprep Si60 sorbents of four different heparin contents (HLC 21a–HLC 21d)

Adsorbent	Low concentration range		High concentration range		Heparin content (mg/ml adsorbent)
	Stoichiometry (mol T–mol H)	K_d (μM)	Stoichiometry (mol T–mol H)	K_d (μM)	
High thrombin (B056: 5279 U/ml)					
HLC 21a	0.11	0.0008	3.19	0.27	0.29
HLC 21b	0.034	0.0003	1.71	0.29	1.12
HLC 21c	0.027	0.0005	1.60	0.47	2.56
HLC 21d	0.021	0.0013	1.10	0.36	8.58
Low thrombin (B062: 43 U/ml)					
HLC 21a	0.06	0.024			0.29
HLC 21b	0.12	0.045			1.12
HLC 21c	0.08	0.033			2.56
HLC 21d	0.06	0.027			8.58

Averages of molar values obtained using the three different linearisation plots are shown.
The top part of the table shows the data for the low and high protein concentration ranges using starting material with high thrombin content (batch B056).
In the bottom part of the table, the average values for the interaction using starting material with low thrombin content (batch B062) are shown.
T = thrombin, H = heparin.

defective or degraded. Either of these explanations would be in accordance with the low specific thrombin activity in batch B062.

3.2. Batch adsorption experiments with heparin–Fractosil 1000 sorbents

3.2.1. Adsorption isotherms

Isotherms describing the interaction in terms of U thrombin/ml sorbent are shown in Fig. 5. Values for q_m and K_d are shown in Table 9. Average molar values are given in Table 10. As evident from Fig. 5 Tables 9 and 10, the quantitative analysis revealed a two-mode interaction with the heparin–Fractosil 1000 sorbent, which was similar to that observed for the heparin–LiChroprep Si60 sorbents. This behaviour was also evident with the commercial heparin–Sepharose. As seen in Fig. 5, the approximate capacity of the HFS 13 sorbent expressed in U/ml was considerably higher than that of commercial heparin–Sepharose. This difference was approximately by a factor of two at both concentration ranges (see Table 9), partly due to the higher heparin content on the HFS 13 sorbent. However, it also reflected a superior ligand accessibility with the heparin–Fractosil 1000 sorbent, which was evident from the 30% higher mol T–mol H stoichiometry with this silica-based sorbent, as seen in Table 10. Thrombin adsorbed onto the commercial heparin–Sepharose with an apparent K_d of 0.73 μM; this value was similar to the apparent dissociation constants reported by other investigators [30,31]. The binding affinity for the adsorption of thrombin onto the heparin–Fractosil 1000 sorbent was slightly lower, as evident from dissociation constants in the range ca. 1.4–2.0 μM. These values were, however, still well within the range of the non-specific electrostatic thrombin–heparin interaction reported by other investigators [32,33].

3.3. Temperature dependence of the heparin–Fractosil 1000 sorbents

As evident from Tables 9 and 10, no major differences in the binding affinity were observed between 4 and 25°C in the high thrombin concentration range for the heparin–Fractosil 1000 sorbents. This result was in accordance with findings from binding equilibrium studies by Olson et al. [35]. The largely electrostatic lower affinity heparin–

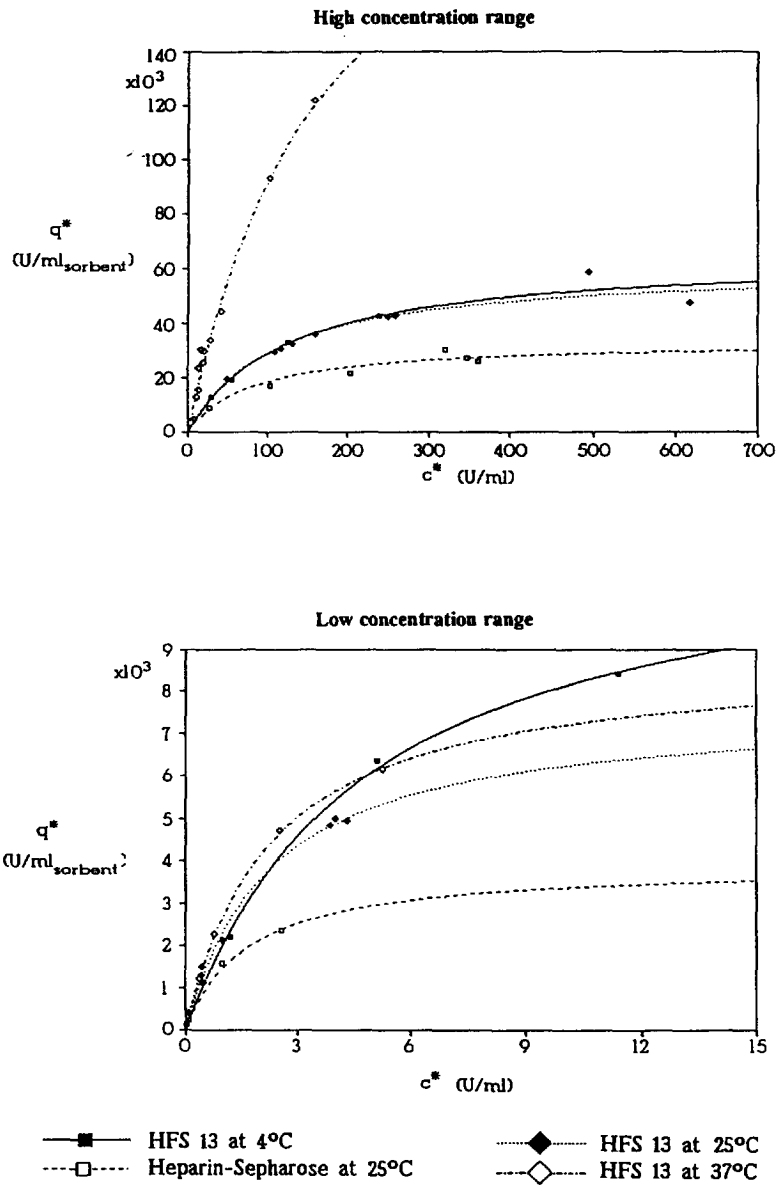

Fig. 5. Isotherms for the adsorption of thrombin with the HFS 13 adsorbent at 4, 25 and 37°C, and the adsorption of thrombin on commercial heparin–Sepharose at 25°C. The adsorption of thrombin (batch B998) on the HFS 13 sorbent was studied through batch adsorption at 4, 25 and 37°C, as described in Section 2. Isotherms were fitted to the data points using the computer software written for this purpose and used for the calculation of the equilibrium parameters (see text). Isotherms for the high and low concentration ranges of the thrombin–heparin interaction are shown.

thrombin interaction is not greatly affected by temperature. At 37°C, however, a large increase in capacity was observed. The adsorption isotherm at 37°C did not show any tendency towards saturation at thrombin–sorbent ratios that resulted in saturation at 25°C. A possible interpretation of this finding could be that the heparin chains are "folded up" along the surface of the sorbent and, therefore, less accessible at lower temperatures, but become extended and much more accessible somewhere between

Table 9
Equilibrium data for the adsorption of thrombin with the HFS 13 adsorbent at 4, 25 and 37°C, and the adsorption of thrombin on commercial heparin–Sepharose at 25°C

Low range Plot	q'_m (U/ml adsorbent)	K'_d (U/ml sorbent)	Stoichiometry (mol T–mol H)	K_d (μM)	Correlation coefficient
HFS 13 (4.15 mg heparin/ml adsorbent), 4°C					
Low range plot					
Double reciprocal	10 400	4.00	0.39	0.047	0.997
Scatchard	122 004	4.97	0.46	0.058	0.982
Scott	12 130	4.94	0.46	0.058	0.997
High range plot					
Double reciprocal	60 950	112	2.30	1.30	0.997
Scatchard	64 600	124	2.45	1.44	0.988
Scott	64 850	124	2.46	1.44	0.998
HFS 13, 25°C					
Low range plot					
Double reciprocal	6400	1.74	0.243	0.020	0.993
Scatchard	7500	2.15	0.285	0.025	0.903
Scott	7600	2.26	0.289	0.026	0.982
High range plot					
Double reciprocal	60 500	110	2.29	1.28	0.991
Scatchard	66 200	135	2.51	1.57	0.927
Scott	60 800	109	2.30	1.27	0.978
HFS 13, 37°C					
Low range plot					
Double reciprocal	9500	2.54	0.36	0.03	0.999
Scatchard	9000	2.34	0.34	0.03	0.996
Scott	8800	2.26	0.34	0.03	0.999
High range plot					
Double reciprocal	463 000	338	17.6	3.94	0.933
Scatchard	256 500	172	9.72	2.00	0.637
Scott	251 500	173	9.53	2.02	0.851
Commercial heparin–Sepharose (2.64 mg heparin/ml adsorbent), 25°C					
Low range plot					
Double reciprocal	2900	1.21	0.174	0.014	0.997
Scatchard	4200	1.80	0.249	0.021	0.964
Scott	4000	1.66	0.234	0.019	0.991
High range plot					
Double reciprocal	26 300	43.3	1.57	0.50	0.987
Scatchard	31 500	64.5	1.88	0.75	0.915
Scott	33 300	80.7	1.98	0.94	0.982

Thrombin batch B998 (1638 U/ml) was used in this study.
Initial maximum capacities and dissociation constants, expressed in terms of activity units per volume, were converted to molar values as described in the text.
Data generated using three different linearisation plots (double reciprocal, Scatchard and semi-reciprocal/Scott) are shown.
The first-order linear correlation of the data to these plots is shown in the last column.
The data have been divided into "high" and "low" protein concentration ranges, representing the two modes of interaction that were observed using a high thrombin content material.
T = thrombin, H = heparin.

Table 10
Average molar equilibrium values for the adsorption of thrombin with the HFS 13 adsorbent at 4, 25 and 37°C, and the commercial heparin–Sepharose at 25°C

Adsorbent	Temperature	Low concentration range		High concentration range		Heparin content
	(°C)	Stoichiometry (mol T–mol H)	K_d (μM)	Stoichiometry (mol T–mol H)	K_d (μM)	(mg/ml adsorbent)
HFS 13	4	0.44	0.054	2.41	1.39	4.15
	25	0.27	0.024	2.37	1.38	
	37	0.35	0.028	9.62	2.01	
Commercial HS	25	0.22	0.018	1.81	0.73	2.64

Averages of molar values in the low and high concentration ranges obtained using the three different linearisation plots (see Table 9) are shown.
T = thrombin, H = heparin, HS = heparin–Sepharose.

25°C and 37°C. This interpretation would contrast with earlier conclusions with regard to the ligand capacity of heparin sorbents, since it suggests a capacity greater than that derived solely on geometrical/steric considerations. A more probable explanation would involve protein–protein interactions that cause multiple layers of thrombin to form at the ligand interface. This behaviour would be in accordance with the observation that the adsorption isotherm lacks saturation at 37°C and can be approximated by a Freundlich-type isotherm [40]. The weaker affinity at 37°C, as evident from the higher K_d value of 2.0 μM, supports this explanation (see Table 10). The explanation involving a multi-layering mechanism was further favoured, since the large increase in capacity at 37°C was not reflected by a significant increase in thrombin–heparin stoichiometry in the low thrombin concentration range. The proposed protein stacking is most likely to occur in the high protein concentration range.

3.4. Critical equilibrium concentrations

The two-modes of interaction described above for the heparin–LiChroprep Si60 and the heparin–Fractosil 1000 sorbents were further explored by determining the equilibrium concentrations at which the dominance of one mode of interaction was replaced by that of the other mode. These concentrations are represented by the intercepts of the two different slopes in double reciprocal, Scatchard, or Scott plots, and are referred to here as the "critical equilibrium concentrations". In this study, calculations were based on the Scott plot, which takes the form

$$c^*/q^* = kc^* + m \tag{4}$$

Intercepts were calculated using the computer-generated regression coefficients (k and m) at the low ($_L$) and high ($_H$) thrombin concentration ranges for each sorbent. This regression analysis was carried out by setting

$$(k_L c_L^*) + m_L = (k_H c_H^*) + m_H \tag{5}$$

and

$$c_L^* = c_H^* = c_{crit}^* \tag{6}$$

From these relationships, it follows that

$$c_{crit}^* = (m_H - m_L)(k_L - k_H)^{-1} \tag{7}$$

whilst substitution of Eq. (1) and Eq. (4) yields

$$q_{crit}^* = c_{crit}^*[(k_L c_{crit}^*) + m_L]^{-1} \tag{8}$$

and

$$q_{crit}^* = (m_H - m_L)(k_L m_H - k_H m_L)^{-1} \tag{9}$$

where m_H, k_H and m_L, k_L = regression coefficients in the high and low concentration ranges; c_L^*, c_H^* = free thrombin concentrations in the high and low concentration ranges; and c_{crit}^* and q_{crit}^* = critical free and bound thrombin concentrations at equilibrium. Eq. (6) was used to calculate the critical equilibrium concentrations of the bound thrombin, which were

Table 11
Calculation of critical equilibrium concentrations for the interaction of thrombin with heparin sorbents

Adsorbent	Heparin content (mg/ml adsorbent)	Concentration range	$k \times 10^3$	$m \times 10^3$	q^*_{crit} (mmol T–mol H)
HLC 19	1.64	Low	1.59	0.21	49.0
		High	0.057	1.08	
HLC 20	1.70	Low	1.00	0.27	83.3
		High	0.06	2.58	
HLC 21a	0.29	Low	4.91	0.23	105
		High	0.16	4.40	
HLC 21b	1.12	Low	4.00	0.10	33.8
		High	0.074	2.58	
HLC 21c	2.56	Low	2.51	0.13	22.9
		High	0.034	2.07	
HLC 21d	8.58	Low	0.94	0.11	15.8
		High	0.016	0.54	
HFS 13, 4°C	4.15	Low	0.083	0.41	377
		High	0.015	1.92	
HFS 13, 25°C		Low	0.13	0.30	247
		High	0.017	1.79	
HFS 13, 37°C		Low	0.11	0.256	213
		High	0.004	0.69	
Comm. HS 25°C	2.64	Low	0.26	0.43	197
		High	0.03	2.42	

The equilibrium concentrations (q^*_{crit}) of adsorbed thrombin at which the low concentration interaction changes to high concentration interaction were determined by calculating the intercepts of the first-order curve-fits for the semi-reciprocal plots for each interaction. The constants k and m represent the regression coefficients of these semi-reciprocal plots.
T = thrombin, H = heparin.

then converted to mmol thrombin/mol heparin as described above. These values are shown in Table 11, together with regression coefficients of Scott plot slopes in the high and low thrombin concentration ranges for the different sorbents.

As evident from Table 11, the critical equilibrium concentration values (q^*_{crit}) reflected the previous observations regarding relative binding site accessibility on heparin–LiChroprep Si60 sorbents with different heparin contents. Thus, for the HLC 21a–HLC 21 sorbents, an inverse proportionality between q^*_{crit} and heparin ligand density (here represented by the heparin content per ml of sorbent) was apparent. Accurate predictions of critical equilibrium concentrations could, however, not be made solely based on the ligand density of the sorbent. Although the ligand densities on the HLC 19 and HLC 20 sorbents were intermediate to those of HLC 21b and HLC 21c, their critical equilibrium concentrations assumed values intermediate to those of the HLC 21a and HLC 21b sorbents. Since two different thrombin starting materials, batches B056 and B995, were used with these sorbents, this finding demonstrated that the critical equilibrium concentration values are influenced by variations in starting material composition.

The macroporous heparin–Fractosil 1000 sorbent (HFS 13) had a heparin content intermediate to that of the mesoporous HLC 21c and HLC 21d sorbents. At 25°C, q^*_{crit} was however approximately ten-times higher than that obtained with the heparin–LiChroprep Si60 sorbents, clearly demonstrating a better ligand accessibility with the larger pore size and greater accessible surface area with the heparin–Fractosil 1000. Similarly, the previously observed 30% higher thrombin–heparin stoichiometry value for the HFS 13 sorbent, relative to commercial heparin–Sepharose, was closely paralleled by a 25% higher q^*_{crit} for the HFS 13 sorbent. An inverse proportionality of q^*_{crit} with temperature was ob-

served for the HFS 13 sorbent. As seen by the high q^*_{crit} at 4°C, these data indicate that the thrombin interaction is favoured at low temperatures.

3.5. Geometric considerations

Stoichiometries (mol thrombin–mol heparin) were calculated using the average value of 13 500 g/mol for the molecular mass of heparin [25]. However, this value oversimplifies the calculations, since the commercial heparin preparation used in the synthesis of the affinity sorbents ranged between 5000 and 30 000 in molecular mass. As an example, the capacity of the HFS 13 sorbent at 25°C was determined to be 65 989 U of thrombin/ml of sorbent, which translated to 2.37 mol T–mol H, when a heparin molecular mass of 13 500 was used in the calculation. If the whole range of heparin's molecular masses were to be incorporated instead, this would translate to a stoichiometric range of 0.88–5.3 mol thrombin–mol heparin.

The average diameter of thrombin can be approximated to 6.2 nm [24], using a formula developed by Janin [41]. The lengths of the heparin molecules range between 6.4 and 42 nm, based on the molecular mass range 5000 to 30 000 g/mol and X-ray diffraction values of the tetrasaccharide fibre axis periodicity of heparin obtained from the literature [42]. The size ratios of heparin lengths to thrombin diameter are thus defined by the range 1.08 to 7.06, which is similar to the experimental molar ratios obtained in this investigation. This apparent correlation between the theoretical and experimental molar ratios suggest that the binding sites on immobilised heparin are entirely accessible to thrombin on the HFS 13 heparin–Fractosil 1000 support and that, as maximum capacity is reached, the thrombin becomes densely packed along the heparin molecule. This concept is visualised schematically in Fig. 6. A similar comparison between experimental results has been presented by Evington et al. [33], based on fluorescence polarisation titrations, which suggested that one thrombin molecule bound to a segment of heparin of M_r 3000. This result was related by Evington et al. [33] to a steric requirement of a 4.2-nm length of heparin for a thrombin molecule with an average diameter of 4.5 nm, as thrombin becomes densely packed along the heparin molecule.

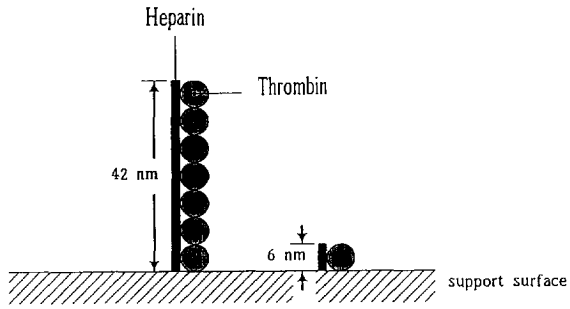

Fig. 6. Schematic representation of the geometric proportions of thrombin and heparin. Schematic representation of heparin molecules with M_r values in the range 5000 to 30 000 are depicted as end-point-attached on a silica surface, with densely packed adsorbed thrombin molecules.

Although the findings of these investigators thus supported the possibility that a dense packing of thrombin on heparin may actually be the case upon saturation of the HFS 13 sorbent, the situation with immobilised heparin will most likely be different to that using heparin in solution.

4. Conclusions

These investigations were aimed at the characterisation of silica-based heparin-affinity sorbents. To achieve optimal binding-site accessibility of the ligand, heparin was end-point-attached through reductive amination onto amino-derivatised LiChroprep Si60 and Fractosil 1000. Due to their radically different pore sizes and specific surface areas, the heparin–LiChroprep Si60 (pore size 60 Å, 500 m^2/g) and heparin–Fractosil 1000 (pore size 1000 Å, 20 m^2/g) sorbents possessed markedly different properties. Firstly, the small pore-size of LiChroprep Si60 restricted the immobilisation of heparin and the interaction with solutes in chromatographic applications to the outer surface area of these silica particles. The heparin–LiChroprep Si60 sorbents thus performed essentially as non-porous affinity sorbents under these circumstances. With the heparin–Fractosil 1000 sorbents, the larger pore size (1000 Å) enabled both the immobilisation of heparin and the solute interaction to take place within the pores to a

much greater extent. The heparin–Fractosil 1000 sorbents thus performed in a manner that was more similar to that of the commercial heparin–Sepharose in this respect. Secondly, the ligand densities of the heparin–LiChroprep Si60 sorbents were very high, resulting in decreased binding-site accessibilities due to steric effects.

With the heparin–Fractosil 1000 sorbents, the ligand densities were much lower, resulting in improved binding site accessibilities. Generally, the heparin–Fractosil 1000 sorbents displayed characteristics that were equal or superior to those of commercial heparin–Sepharose with regards to capacity and ligand accessibility. Thus, the HFS 13 heparin–Fractosil 1000 sorbent bound 2.34 mol of thrombin (T) per mol of heparin (H), compared to 1.79 mol T–mol H on commercial heparin–Sepharose and 1.49 mol T–mol H on the HLC 20 heparin–LiChroprep Si60 adsorbent. Although the ligand accessibility was lower with the heparin–LiChroprep Si60 sorbents, these sorbents nevertheless had some advantages due to the absence of mass-transfer resistance effects associated with pore diffusion.

The batch data with thrombin suggested two modes of thrombin–heparin interaction on the heparin sorbents. A weaker interaction at higher equilibrium concentrations, with dissociation constants (K_d) in the micromolar range, matched literature data for a non-specific electrostatic interaction well. A higher-affinity interaction, with K_d values in the nanomolar range, was evident at very low concentrations. Such an interaction has also been suggested by other investigators [36,38].

Acknowledgments

These investigations were supported by a grant from the Industrial Research and Development Board of the Department of Industry, Trade and Regional Development. Silica-based chromatographic support materials were kind gifts from E. Merck, Darmstadt, Germany. The provision of protein materials by the Blood Products Division, CSL, Victoria, Australia, is gratefully acknowledged. M.T.W. Hearn also acknowledges the receipt of an Alexander Von Humboldt Forschungspreis

References

[1] J. Hoffman, O. Larm and E. Scholander, Carbohydr. Res., 117 (1983) 328.
[2] O. Larm, R. Larsson and P. Olsson, in D.A. Lane and U. Lindahl (Editors), Heparin, Chemical and Biological Properties, Clinical Applications, Edward Arnold, London, 1989.
[3] R.J. Linhardt, Chem. Ind., 2 (1991) 45.
[4] P.-H. Iverius, Biochem. J., 124 (1971) 677.
[5] P.W. Gentry and B. Alexander, Biochem. Biophys. Res. Commun., 50 (1973) 500.
[6] I. Danishefsky, F. Tzeng, M. Ahrens and S. Klein, Thromb. Res., 8 (1976) 131.
[7] B. Nordenman and I. Björk, Thromb. Res., 11 (1977) 799.
[8] M. Miller-Andersson, H. Borg and L.-O. Andersson, Thromb. Res., 5 (1974) 439.
[9] H. Sasaki, A. Hayashi, H. Kitagaki-Ogawa, I. Matsumoto and N. Seno, J. Chromatogr., 400 (1987) 123.
[10] M. Funahashi, I. Matsumoto and N. Seno, Anal. Biochem., 126 (1982) 414.
[11] K.K. Unger (Editor), Packings and Stationary Phases in Chromatographic Techniques (Chromatographic Science Series, Vol. 47), Marcel Dekker, New York, 1990.
[12] M. Miller-Andersson, P.J. Gaffney and M.J. Seghatchian, Thromb. Res., 20 (1980) 109.
[13] M.J. Seghatchian, M. Miller-Andersson and P. Gaffney, Thromb. Haemostas., 38 (1977) 218.
[14] D.J. Winzor, P.D. Munro and C.M. Jackson, J. Chromatogr., 597 (1992) 57.
[15] S.T. Olson, P.E. Bock and R. Sheffer, Arch. Biochem. Biophys., 286 (1991) 533.
[16] M. Hoylaerts, W.G. Owen and D. Collen, J. Biol. Chem., 259 (1984) 5670.
[17] U. Abildgaard, M. Lie and O.R. Ødegård, Thromb. Res., 11 (1977) 549.
[18] G. Axelsson, K. Korsan-Bengtsen and J. Waldenström, Thromb. Haemost., 36 (1976) 517.
[19] F.B. Anspach, A. Johnston, H.-J. Wirth, K.K. Unger and M.T.W. Hearn, J. Chromatogr., 476 (1989) 205.
[20] F.L. Zhou, D. Muller, X. Santarelli and J. Jozefonvicz, J. Chromatogr., 476 (1989) 195.
[21] F.L. Zhou, D. Muller and J. Jozefonvicz, J. Chromatogr., 510 (1990) 71.
[22] Kabi Diagnostica AB. S2238 — Determination of Antithrombin–Heparin Cofactor in Plasma (Laboratory Instruction). Kabi Diagnostica, Stockholm, Sweden, 1985.
[23] K.K. Unger, in K.K. Unger (Editor), Packings and Stationary Phases in Chromatographic Techniques, Marcel Dekker, New York, 1990, pp. 235–250.
[24] M. Björklund and M.T.W. Hearn, J. Chromatogr. A, 729 (1996) 149.
[25] J.E. Dyr and J. Suttnar, J. Chromatogr., 563 (1991) 124.
[26] J.W. Fenton, II, M.J. Fasco, A.B. Stackrow, D.L. Aronson, A.M. Young and J.S. Finlayson, J. Biol. Chem., 252 (1977) 3587.
[27] M. Björklund and M.T.W. Hearn, J. Chromatogr. A, 743 (1996) 145.

[28] A.R. Thompson and E.W. Davie, Biochim. Biophys. Acta, 250 (1971) 210.
[29] G. Schmer, Hoppe-Seyler's Z. Physiol. Chem., 353 (1972) 810.
[30] S.T. Olson, J. Biol. Chem., 263 (1988) 1698.
[31] R.E. Jordan, G.M. Oosta, W.T. Gardner and R.D. Rosenberg, J. Biol. Chem., 255 (1980) 10073.
[32] J.R.N. Evington, P.A. Feldman, M. Luscombe and J.J. Holbrook, Biochim. Biophys. Acta, 870 (1986) 92.
[33] J.R.N. Evington, P.A. Feldman, M. Luscombe and J.J. Holbrook, Biochim. Biophys. Acta, 871 (1986) 85.
[34] M. Nesheim, M.N. Blackburn, C.M. Lawler and K.G. Mann, J. Biol. Chem., 261 (1986) 3214.
[35] S.T. Olson, H.R. Halvorson and I. Björk, J. Biol. Chem., 266 (1991) 6342.
[36] M.J. Griffith, H.S. Kingdon and R.L. Lundblad, Arch. Biochem. Biophys., 195 (1979) 378.
[37] M.J. Griffith, J. Biol. Chem., 254 (1979) 12044.
[38] Y. Byun, H.A. Jacobs and S.W. Kim, ASAIO J., 38 (1992) 649.
[39] H.-J. Wirth, K.K. Unger and M.T.W. Hearn, J. Chromatogr., 550 (1990) 383.
[40] H. Freundlich, Colloid and Capillary Chemistry, Methuen and Co., London, 1926.
[41] J. Janin, Nature, 277 (1979) 491.
[42] E.D.T. Atkins, D.H. Isaac, I.A. Nieduszynski, C.F. Phelps and J.K. Sheehan, Polymer, 15 (1974) 263.
[43] G.M.S. Finette, Q.M. Mao and M.T.W. Hearn, J. Chromatogr. A, (1997) in press.